# Improvement of the Strength of a Novel Shear Web Blade Design by Numerical Analysis

Firlya Rosa[1,2*], Tubagus Ahmad Fauzi Soelaiman[1], Priyono Soetikno[1], I Wayan Suweca[1], and Mochammad Agoes Moelyadi[1]
[1]Mechanical Engineering Study Program
Bandung Institute of Technology
Bandung, 40132 Indonesia
**f105a@yahoo.com*

[2]Department of Mechanical Engineering
Universitas Bangka Belitung
33172 Indonesia

Date received: May 20, 2024
Revision accepted: November 3, 2025

## Abstract

*The geometry of a shear web significantly affects the performance of wind turbines. This study investigates the mechanical behavior of novel shear web configurations inspired by banana leaf midrib topology, compared to conventional designs. Finite Element Method (FEM) and Fluid-Structure Interaction (FSI) simulations were employed to evaluate stress distribution, deflection, and modal frequencies under varying wind speeds (3–7 m/s). The aerodynamic forces acting on the blade were derived from airfoil profiles inspired by banana leaf midribs. Results show that the blade with a short banana leaf midrib shear web achieved the lowest deflection, while the long midrib configuration minimized stress. Additionally, the dual-web configuration exhibited the lowest natural frequencies. These findings demonstrate that biomimetic shear web designs can enhance structural efficiency and offer promising alternatives to conventional blades.*

***Keywords**:* blade stress, deflection, low wind speed, plant topology, shear web

## 1. Introduction

The structural performance of wind turbine blades is significantly influenced by internal components such as shear webs, which serve as the primary support elements against bending and torsional loads induced by wind. Various optimization strategies have been developed to reduce blade mass and enhance stiffness; however, most studies still focus on conventional geometries with one or two shear webs arranged perpendicular to the blade chord. While these approaches have proven effective in some instances, their

structural efficiency remains limited—particularly for medium-scale turbines operating in low-wind-speed regions.

Several studies have explored variations in the number and shape of shear webs (J.W. Liu, *et al*., 2022; Balokas & Theotokoglou, 2018; Zhang *et al.* 2023; Zhu *et al*., 2020; Zhu *et al*., 2016), including the use of three-web (Hayat *et al*., 2022; Yang *et al*., 2019) and honeycomb-like structures (W. Liu *et al*., 2022). However, findings suggest that increasing the number of shear webs does not always lead to significant improvements in mechanical performance and may even reduce torsional stiffness (Sharma *et al*., 2021). Therefore, alternative approaches are needed that not only reduce mass but also optimize load distribution.

Biomimetic design offers promising solutions to this challenge. Natural structures such as leaf venation systems have demonstrated efficient load distribution with minimal material usage. Several researchers have explored plant-inspired topologies for shear web design (Liu *et al*., 2009; Wang-yu & Yong, 2010), but applications have been mainly limited to generic forms and have not yet addressed specific structures such as banana leaf midribs. Momeni *et al*. (2019) showed that shear web geometries adapted from plant leaf structures can improve static stiffness, internal strain energy, and fatigue life compared to conventional blade designs. Similarly, the review conducted by Omidvarnia and Sarhadi (2024) highlights that plant biomechanics principles—particularly the structure and function of leaves—have inspired modern wind turbine designs. These designs enable the production of blades that are lighter, stronger, and more resistant to dynamic loads, while also reducing the risk of failure due to material fatigue.

The banana leaf midrib features a hollow structure with longitudinal reinforcements and a curved, arch-like form. This structure has been shown to resist bending and torsional loads effectively in biological-scale mechanical tests (Ennos *et al*., 2000; Wolff-Vorbeck *et al*., 2019). However, no study has explicitly evaluated the mechanical performance of banana leaf midrib-inspired shear web configurations in the context of numerical simulations for wind turbine blades, particularly under low wind speed conditions typical in tropical regions such as Indonesia.

This study aims to address this gap by evaluating the mechanical performance of several shear web configurations inspired by banana leaf midrib topology. The analysis is conducted using the Finite Element Method (FEM) and one-

way Fluid-Structure Interaction (FSI) simulations to assess stress distribution, deflection, and dynamic behavior of the blade under wind speeds ranging from 3 to 7 m/s. This approach follows the methodology of Nebiewa *et al*. (2026), who conducted a comprehensive one-way FSI analysis on small-scale HAWT blades and validated their CFD-FEA model with experimental data, achieving a correlation of 93%. This study also builds upon a previous investigation by Rosa *et al*. (2022a), which developed an airfoil profile inspired by the morphology of banana leaf midribs and demonstrated promising aerodynamic performance, including a glide ratio of 123.07 at a 2° angle of attack. By comparing the simulation results of biomimetic and conventional shear web designs in terms of mechanical behavior—such as deflection, static stress distribution, and modal dynamics—this study aims to identify potential improvements in structural efficiency applicable to medium-scale wind turbine blades operating in low-wind-speed environments.

## 2. Methodology

### *2.1 Validation of airfoil and blade model*

This study adopts an airfoil previously investigated by Rosa *et al*. (2022a), as depicted in Figure 1a, which was explicitly designed to replicate the cross-sectional morphology of a banana leaf midrib. Numerical simulations were executed in two dimensions, using refined tetrahedral meshes near the airfoil surface and hexahedral meshes within the surrounding fluid domain. For simulation, fluid properties were held constant, with a density of 1.225 kg/m³ and a dynamic viscosity of $1.7894 \times 10^{-5}$ kg/(m·s). A comparison of the lift and drag coefficients (Cl and Cd), obtained using the Blade Element Momentum (BEM) method, is presented in Figure 1b to demonstrate the aerodynamic performance characteristics of the proposed airfoil.

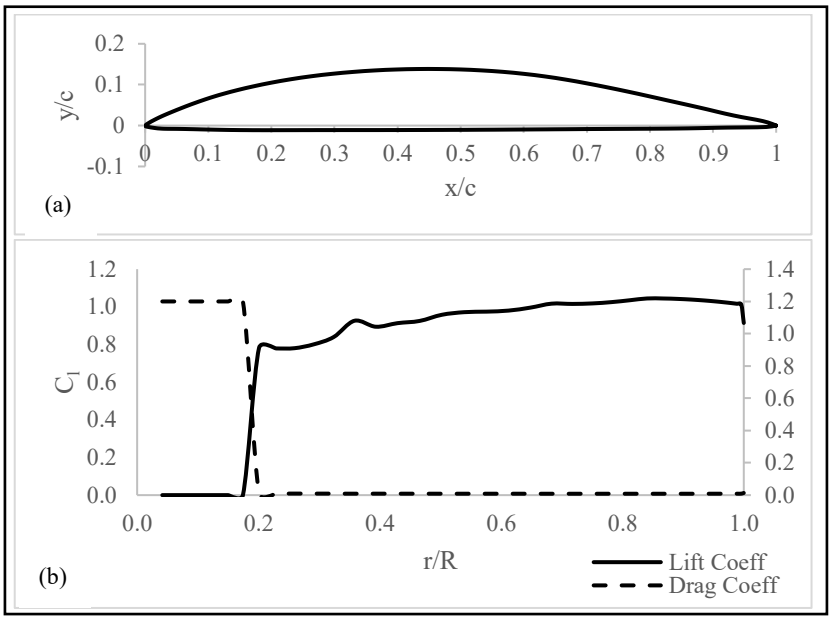


Figure 1. Airfoil profile (Rosa *et al*., 2022a, 2022b) (a); lift and drag coefficients (b)

Based on the aerodynamic data obtained using the BEM method, aided by the QBlade software V.16, blade geometries with six sections were generated Figure 2a. Based on 3D visualization, each section has the highest twist angle at the blade root, and it grows smaller toward the blade tip, following the wind direction (Figure 2b and Figure 2c), and the chord line size and angle of attack of each section can be seen in Figure 2d.

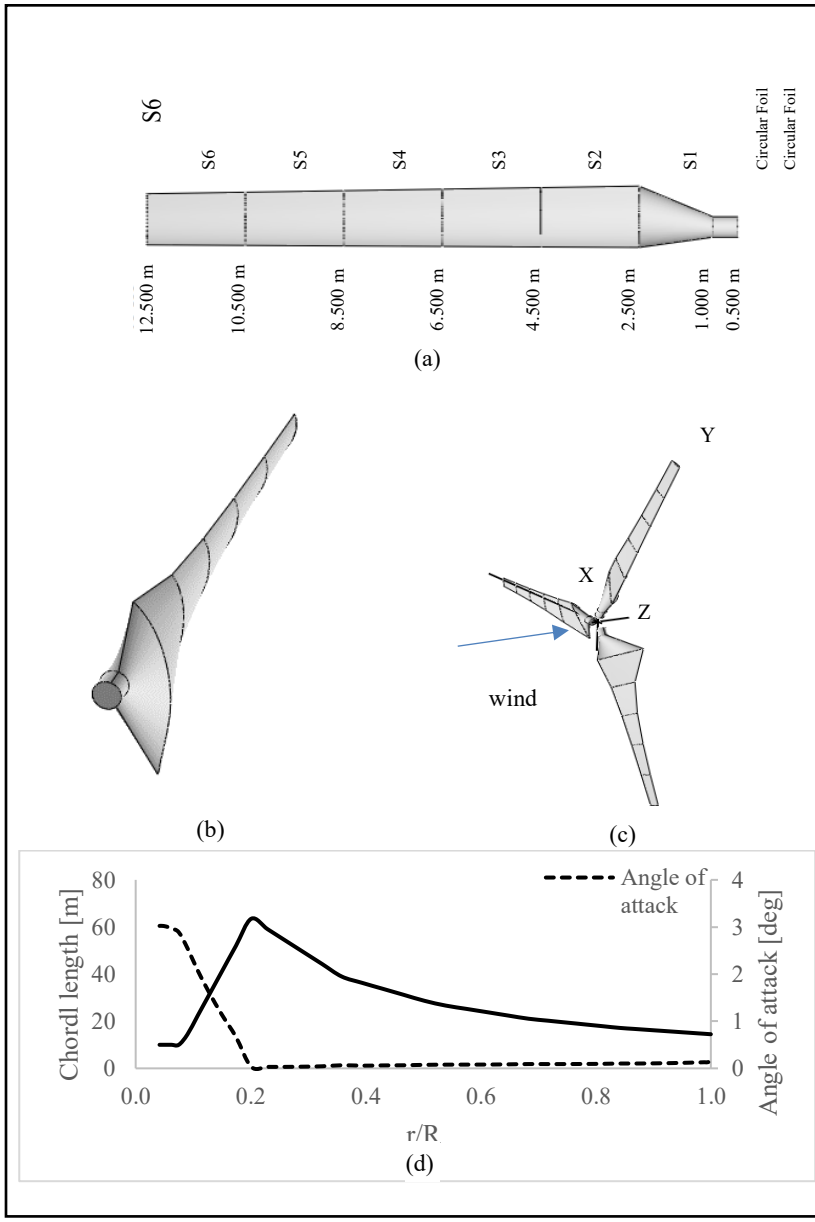


Figure 2. Lengths of the sections of the blade (a); geometry of the blade (b); geometry of the rotor (c)

### *2.2 Validation of CFD model*

This work aims to perform a comprehensive structural analysis of the blade through simulations using the Spalart-Allmaras turbulence model, focusing on both its static structural properties and the dynamic modal responses caused by aerodynamic forces. The cumulative forces obtained via simulations using Ansys Fluent were integrated employing the Fluid-Structure Interaction (FSI) methodology, with primary parameters detailed in Table 1. Additionally, the Blade Element Momentum (BEM) approach was utilized to calculate Reynolds numbers for each sectional segment, as illustrated in Figure 3a.

Table 1. Main parameters

| Parameter | Values | Unit |
|---|---|---|
| Number of blades | 3 | N/A |
| Wind speed working | 3 - 7 | m/s |
| Rotor radius (R) | 12.5 | m |

The FSI modeling in this study adopts a one-way coupling methodology. Initially, the fluid domain is resolved through Computational Fluid Dynamics (CFD) simulations until convergence criteria are satisfied. The aerodynamic pressure distributions obtained are subsequently imposed as boundary load conditions on the Finite Element Analysis (FEA) model. The FEA framework then calculates the structural responses of the blade, including the resulting deformations and stress distribution induced by aerodynamic forces.

The aerodynamic simulations were conducted under parameters and boundary conditions comprehensively delineated in Rosa *et al*. (2025). This reference provides a detailed description of the CFD simulation setup, including domain dimensions, inlet velocity, outlet pressure boundary conditions, wall treatments, mesh configuration, and assumptions such as incompressible and steady-state flow. For the sake of completeness, a succinct overview of the primary simulation framework and assumptions is also presented herein. The CFD results referenced correspond to the operational conditions articulated in Rosa *et al*. (2025), as illustrated in Figure 3b, Figure 3c, and Figure 3d, and were validated using established analytical techniques.

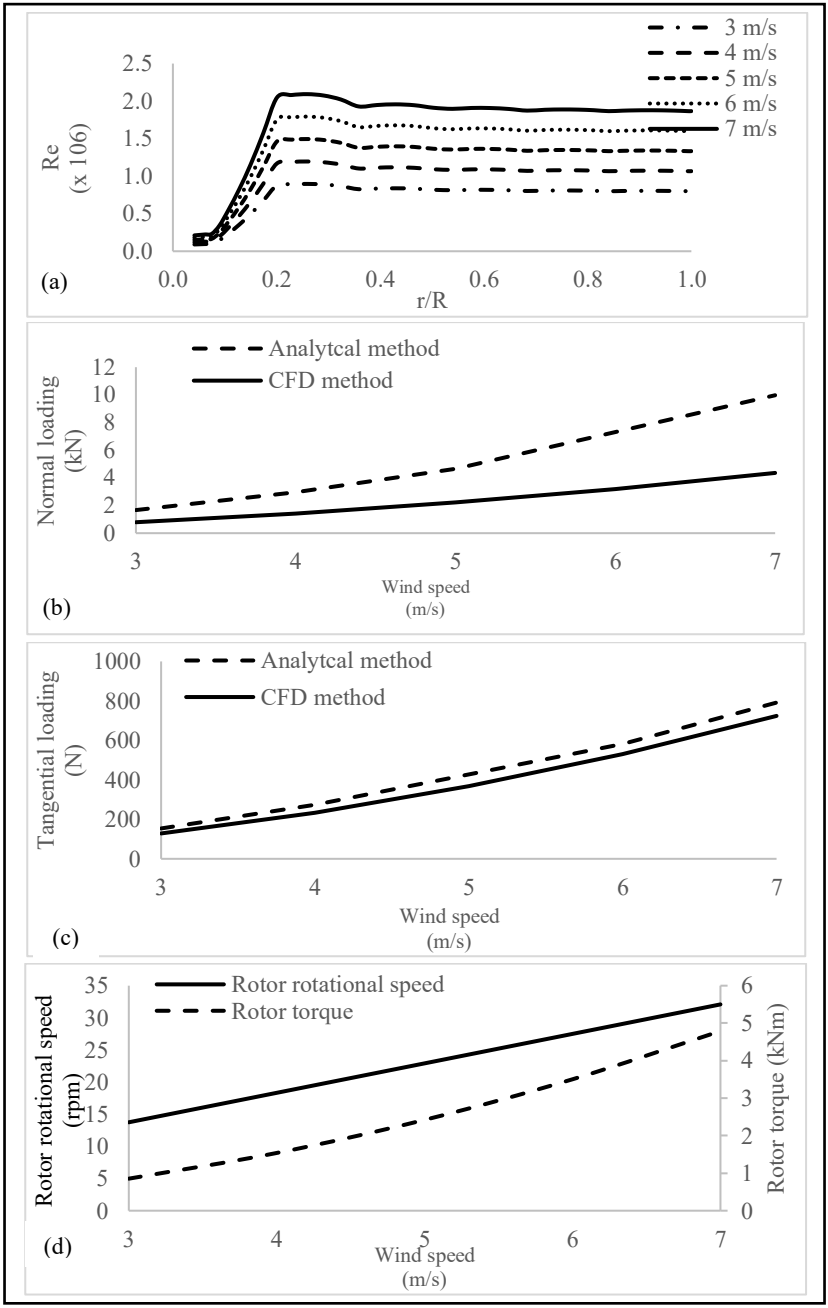


Figure 2. Reynolds number along the blade (a); normal loading on the blade (b); tangential loading on the blade (c); and torque at rotor (d)

Figure 3b and Figure 3c illustrate the tangential force along the y-axis (Ft) and the normal force along the z-axis (Fn), respectively. As depicted in Figure 3d, at a wind speed of 3 m/s, the torque reaches 858.14 Nm with a rotor speed of 13.75 rpm, which significantly increases to 4788.94 Nm at a rotor speed of 32.09 rpm when the wind speed rises to 7 m/s. This increase in torque indicates that the wind turbine system can generate more energy at higher wind speeds, suggesting the potential for enhanced energy conversion efficiency. These findings contribute to a deeper understanding of the structural dynamics of horizontal-axis wind turbines and are expected to serve as a valuable reference for the development of renewable energy technologies.

### *2.3 Alternative blade shear web designs*

This study proposes several alternative shear web geometries for wind turbine blades inspired by the topology of the banana leaf midrib, serving as variations to the conventional shear web design (Figure 4a, Table 2). In the conventional design, shear web-1 is positioned at 25% of the chord length, while shear web-2 is located at 75%. In contrast, the banana leaf midrib-inspired design relocates shear web-2 to 50% of the chord length (Figure 4g). For alternatives Alt-1 and Alt-4, the shear web extends from 25% to 50% of the chord length, whereas in Alt-2, the shear web spans a shorter range from 25% to 30%.

Table 2. Alternative shear web designs

| Name | Symbol | Shear web Forms | Number of Shear webs | Shown on |
|---|---|---|---|---|
| Design alternative 1 | Alt-1 | Banana leaf midrib topology with an arc position starting from the top surface of the air foil | 1 | Figure 4d |
| Design alternative 2 | Alt-2 | Banana leaf midrib topology with a short structure | 1 | Figure 4c |
| Design alternative 3 | Alt-3 | Perpendicular to the chord line | 1 | Figure 4f |
| Design alternative 4 | Alt-4 | Banana leaf midrib topology with an arc position starting from the top surface of the airfoil | 2 | Figure 4b |
| Design alternative 5 | Alt-5 | Perpendicular to the chord line | 2 | Figure 4e |

The selection of these shear web design alternatives is informed by a combination of literature review findings on load distribution efficiency, particularly those highlighted in the work of Omidvarnia and Sarhadi (2024), which demonstrate the superior stiffness and stability of plant-inspired biomimetic configurations. The banana leaf midrib morphology was adopted based on evidence from plant biomechanics, which shows that such natural architectures efficiently distribute loads with minimal material use. The reasoning behind the choice of each alternative is elaborated further in the comparative analysis section.

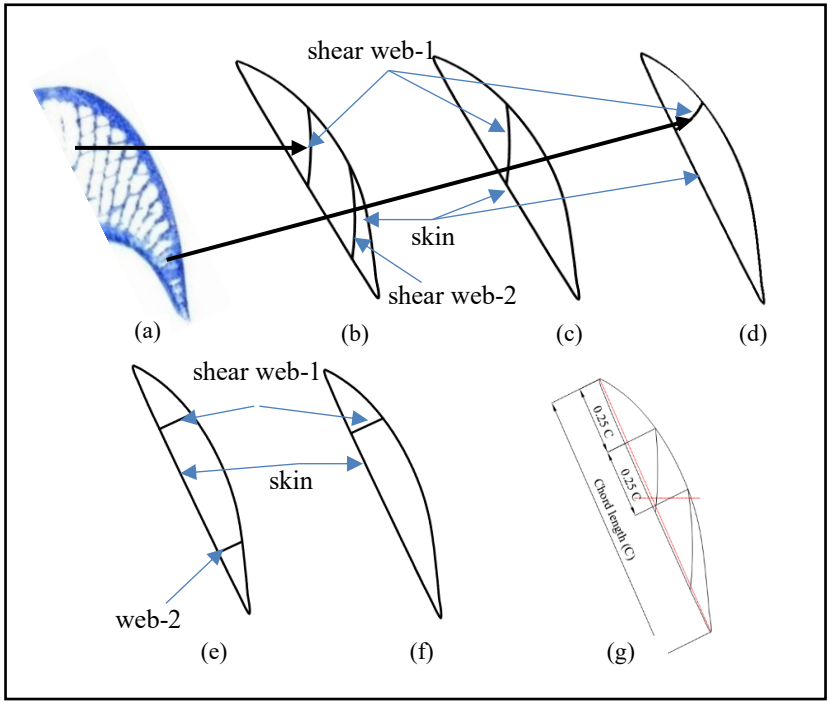


Figure 3. Blade structure modeling (a); alt-4 (b); Alt-2 (c); Alt-1 (d); Alt-5 (e); Alt-3 (f); and shear web positioning (g)

Understanding the impact of these geometric variations is crucial for assessing their influence on blade structural performance. Accordingly, Figure 4 illustrate six alternative blade structural configurations that integrate banana leaf midrib topology with conventional shear web designs. Table 2 details the names and descriptions of these alternatives. Specifically, Alt-1, Alt-2, and Alt-4 adopt the banana leaf midrib topology, with Alt-4 uniquely incorporating two shear webs. Conversely, Alt-3 and Alt-5 retain conventional

shear web structures oriented perpendicular to the chord line. This investigation aims to provide comprehensive insights into how such topological variations may affect the mechanical characteristics and reliability of wind turbine blades.

The modeling of the blade was carried out using the Finite Element Method (FEM) in the Ansys software, focusing on the blade surface and structure. Various thicknesses were applied to the blade surface and structure, ranging from 15 mm at the root to 10 mm at the tip, with the thickness distribution of the skin and shear web depicted in Figure 5a. The graph displays the variations of twist angles based on the blade optimization results obtained by Rosa *et al*. (2022), a previous study using the QBlade software.

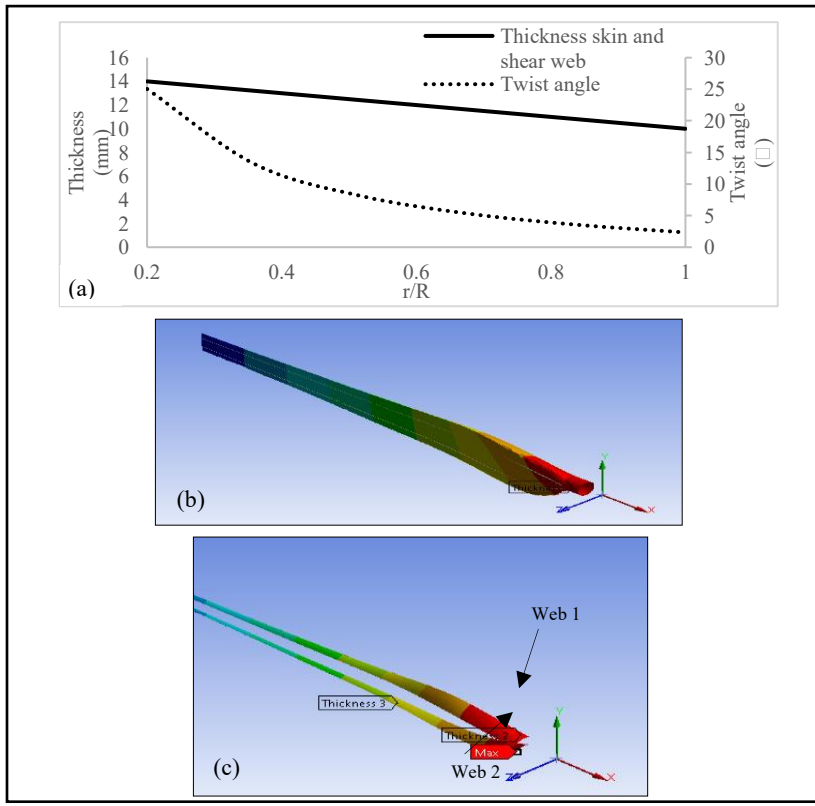


Figure 4. Thickness and twist angle spread (a); skin thickness modeling (b); blade shear web thickness modeling (c)

Meanwhile, Figure 5b and Figure 5c illustrate the modeling of the skin and blade shear web. This methodology allows for a comprehensive examination of thickness and shape differences, which can improve the performance and efficiency of horizontal-axis wind turbines.

### *2.4 Masses of alternative designs*

The blade surfaces of all alternatives are of the same thickness, resulting in the same mass being produced for the surface. The difference lies in the lengths and numbers of the shear webs used, which will affect the overall mass of the blade. The mass for each alternative shear web design is shown in Figure 6. Of the five alternatives, Alt-3 has the smallest mass due to its relatively shorter geometric shear web dimensions, followed by Alt-2. Regarding the blade supported by two shear webs, Alt-5 has the smallest mass due to its short shear webs.

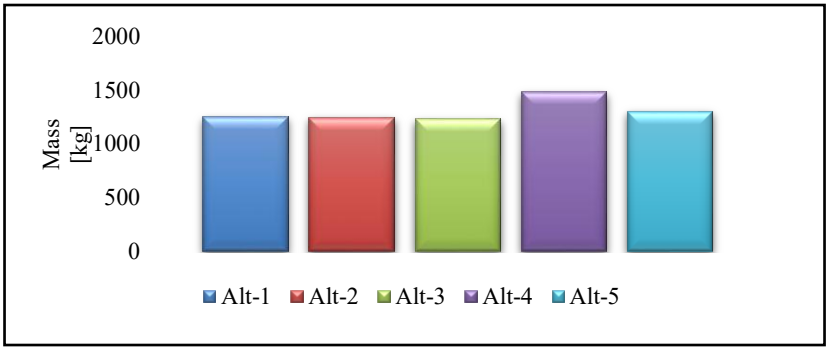


Figure 6. Blade mass by shear web alternative

### *2.5 Blade modeling*

Finite element analysis (FEA) modeling was carried out in several critical stages, including material determination, element selection, boundary condition selection, load determination, and mesh convergence and validation.

#### 2.5.1 Material determination

The blade material is glass-fiber-reinforced polymer (GFRP) with specific properties as listed in Table 3 (Liu & Gong, 2011).

Table 3. Material properties

| Properties | Unit | Value |
|---|---|---|
| Density | g/cm$^3$ | 1,25–2,50 |
| Coefficient of thermal expansion | 10$^{-6}$/°C | 6,0–10,0 |
| Young's modulus | GPa | 35–86 |
| Poisson's ratio | - | 0,33 |
| Bulk modulus | Pa | 2,92E+10 |
| Shear modulus | GPa | 12,5 |
| Tensile ultimate strength | MPa | 483–4580 |

### 2.5.2 Element selection

A program-controlled meshing approach was employed, using a global mesh size of 2 m and seven variations of face mesh sizes on the blade surface: 0.0075 m, 0.0100 m, 0.0150 m, 0.0200 m, 0.0250 m, 0.0300 m, and 0.0400 m. The mapped face meshing adhered to the standard protocols available in Ansys software. The meshing results for the blade surface and shear web are presented in Figure 7a and Figure 7b, respectively.

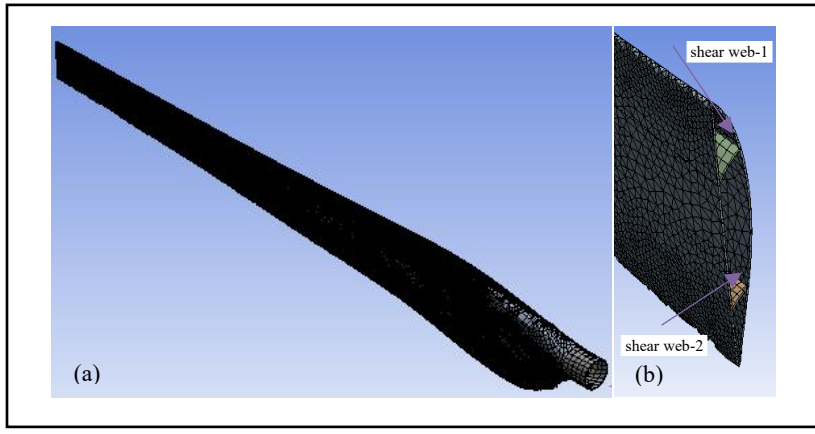


Figure 5. Meshing results on the model (case Alt-4) blade surface (a); and blade shear web (b)

Given the critical importance of meshing quality in wind turbine structural analysis, this study conducted a thorough mesh independence assessment, primarily focusing on the face meshing of the airfoil surface and blade shear web of the second alternative (Alt-2) blade design. Initially, the global mesh size was fixed while the face mesh size was varied.

Mesh quality was evaluated based on skewness and aspect ratio metrics, with all skewness values falling below 0.25, indicating excellent mesh quality. The aspect ratio values approached 1 as the face mesh size decreased, as summarized in Table 4.

Table 4. Mesh quality values based on face mesh size variations

| The meshing of the blade surface | | Meshing quality value | |
|---|---|---|---|
| Global Meshing | Face Meshing | Skewness | Aspect Ratio |
| 2.00 | 0.0075 | 0.05539 | 1.70020 |
| | 0.0100 | 0.05745 | 1.99360 |
| | 0.0150 | 0.05005 | 2.80950 |
| | 0.0200 | 0.05066 | 3.77510 |
| | 0.0250 | 0.04245 | 4.65250 |
| | 0.0300 | 0.05096 | 6.17750 |
| | 0.0400 | 0.05165 | 8.07650 |

The independence criteria were quantitatively assessed by monitoring the convergence of key output parameters, including deflection, force along the z-axis, and maximum stress on the airfoil and blade shear web of Alt-1. Convergence was observed to commence at a face mesh size of 0.01 m (Figure 8a, Figure 8b, and Figure 8c). Beyond this mesh resolution, changes in the monitored parameters became negligible (<1%), thus establishing 0.01 m as an optimal and reliable mesh size for subsequent structural analysis.

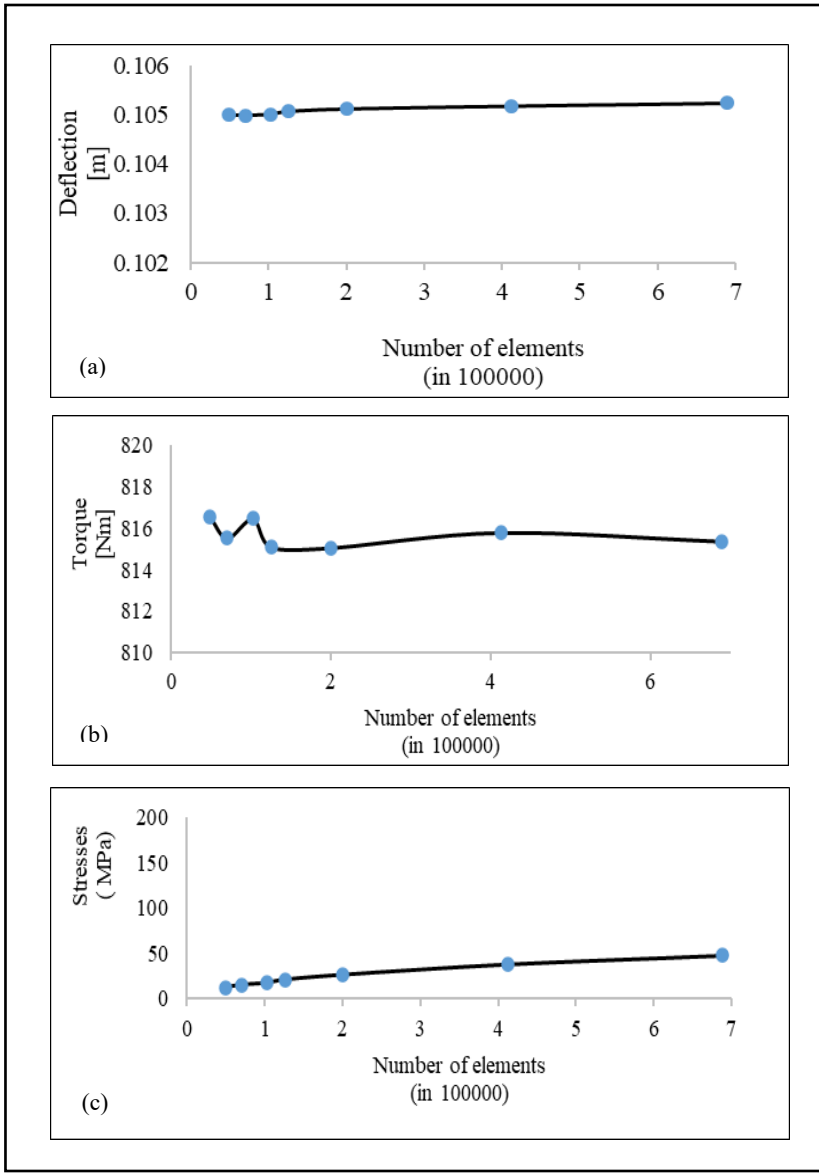


Figure 8. Deflection convergence (a); torque convergence (b); stress convergence (c)

### 2.5.3 Boundary condition selection

The wind turbine blade was represented as a cantilever beam in this simulation, with one end—the root—completely fixed (clamped boundary

condition) and the other end free. This configuration accurately represents the actual attachment of the blade to the wind turbine hub.

Aerodynamic loads on the blade were obtained from CFD simulations at wind speeds ranging from 3 to 7 m/s and subsequently mapped as distributed surface pressure along the blade in the FEA model. These loads were applied in accordance with the local flow vector direction on the blade surface, as illustrated in Figure 9. Gravitational and centrifugal forces were considered negligible due to the assumption of minimal blade mass, but may be applied as distributed loads along the blade axis if required.

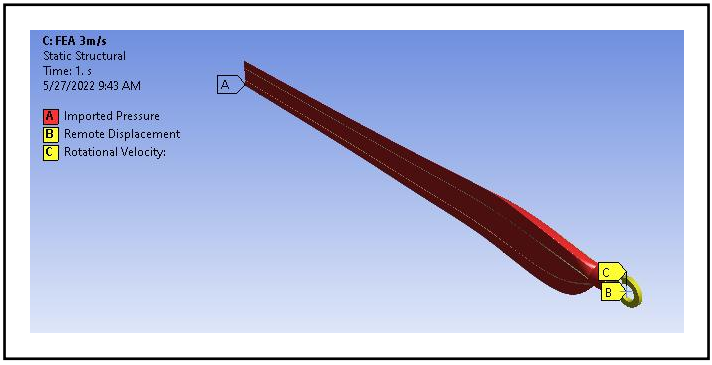


Figure 6. Boundary conditions applied to the blade

2.5.4 Load determination

Mesh-to-mesh interpolation was used to transmit data from CFD to FEA, ensuring accurate aerodynamic pressure distribution mapping onto the structural mesh. Validation of the transfer process was conducted by comparing the total aerodynamic force and pressure distribution before and after mapping, confirming that no significant data loss or distortion occurred. This process ensures the stability and accuracy of the data used in the structural analysis.

*2.6 Static structural and dynamic modal analyses*

The performance of each alternative shear web profile was analyzed using the Ansys Structural and Ansys Dynamic Modal software by applying the single reference frame (SRF) method. In static structural or dynamic modal analysis, single reference frame (SRF) modeling means the analyzed system is

considered a single entity without considering deflection or rotation with respect to other reference systems. It is a common approach in many simulations to simplify structural and modal analysis and optimize computation time.

The variables defined included wind speed and blade angular velocity. To ensure consistent treatment for all blades, the mass of the blade was assumed to be negligible. The analysis results included deflection, stress, reaction moment at the pedestal, reaction force at the pedestal, blade frequency, and deflection under the four-mode condition. The analysis compared the blades with a banana leaf midrib topology airfoil to those with a conventional airfoil.

## 3. Results and Discussion

### *3.1 Static structural analysis*

In this static structural analysis, the blade was treated as a cantilever beam loaded with pressures determined through the aerodynamic analysis as shown on Figure 10a.

#### 3.1.1 Deflection

The deflection moved in the direction of the wind, as shown in Figure 12a. Regarding blades with two shear webs, the highest total deflection at the 7 m/s wind speed occurred in Alt-5, which was not much different from the deflection in Alt-4 Figure 10b, the higher the wind speed, the lower the banana leaf midrib topology shear web deflection. The lowest deflection happened in Alt-4. This was because the Alt-4 cross-section had a more significant moment area inertia than the Alt-5 cross-section.

As for the blades with one shear web, the lowest total deflection occurred in Alt-2. The same was true for the deflection value, there was no significant difference between Alt-1 and Alt-2 because the moments of inertia of the two alternatives were not much different. The smallest total deflection at the 7 m/s wind speed was recorded in Alt-2, with a value of 0.356 m or 35.6 mm.

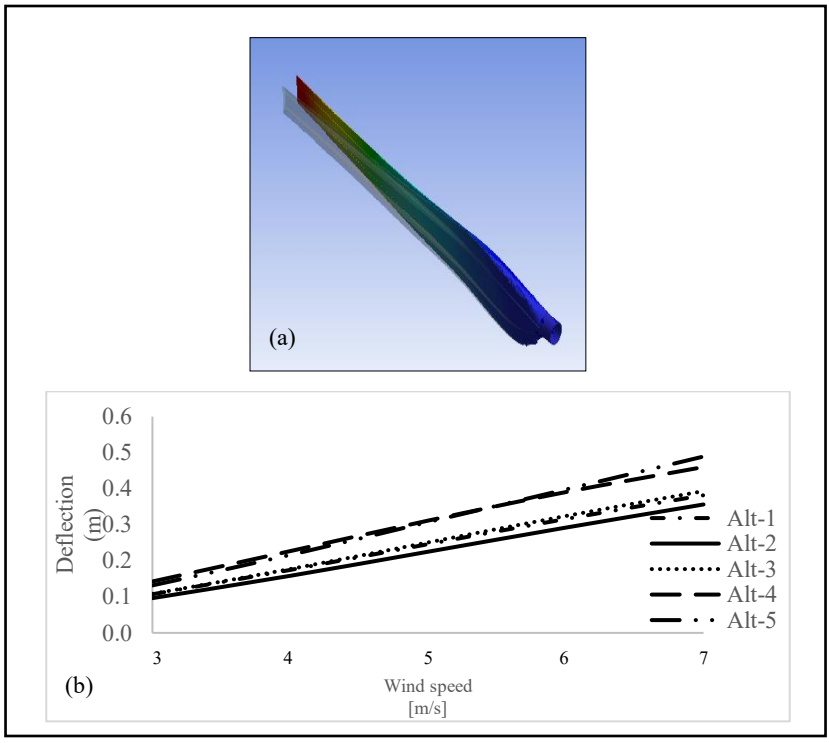


Figure 10. Direction of blade deflection (a) and deflection variation for different design alternatives (b)

However, the difference in total deflection values among all design alternatives was insignificant. The deflections for all design alternatives did not exceed 20% of the rotor radius, as concluded in previous research (Det Norske Veritas, & Risø National Laboratory, 2002). This indicates that the banana leaf midrib topology shear web blade deflects better than the conventional shear web blade.

### 3.1.2 Stresses

Figure 11 illustrates the stress conditions: on the airfoil surface (a), shear web-1 (b), and shear web-2 (c). At the 7 m/s wind speed, the highest stress on the skin occurred in Alt-5, while the lowest occurred in Alt-2, which was not much different from the stress on the skin in Alt-3 (Figure 12a).

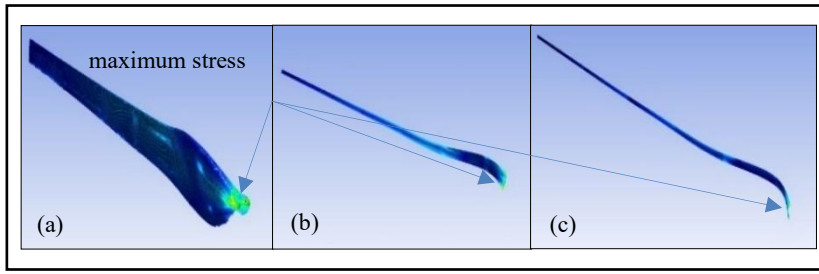


Figure 7. Stress on the skin (a); shear web-1 (b); and shear web-2 (c)

For blades supported by a single shear web, the highest stress on the shear web occurred in Alt-5 at the 7 m/s wind speed, while the lowest stress occurred in Alt-1. The forces that occurred became more prominent as the wind speed increased, although they remained relatively small. Figure 12 illustrates the forces overload the airfoil (a), shear web-1 (b), and shear web-2(c), causing stress in these parts. For the airfoils supported by two shear webs, the stress on Alt-4 was higher than the stress on Alt-5.

From these results, it can be concluded that for the same thickness and mass, shear web-2 in Alt-5 is better than shear web-2 in Alt-4. Based on the yield strength values for the GFRP material presented in Table 3, the airfoil surface thickness, shear web-1 thickness, and shear web-2 thickness had safety factor (SF) values that far exceeded the standardized safety factor values. Based on considerations of masses, deflections, and stresses that occurred on the airfoil, shear web-1, and shear web-2, Alt-2 is a viable option for further research. This decision is supported by the increase in blade mass and the torque value generated from the aerodynamic analysis. It can be concluded that the blade has the potential to reduce the angular acceleration occurring in the turbine.

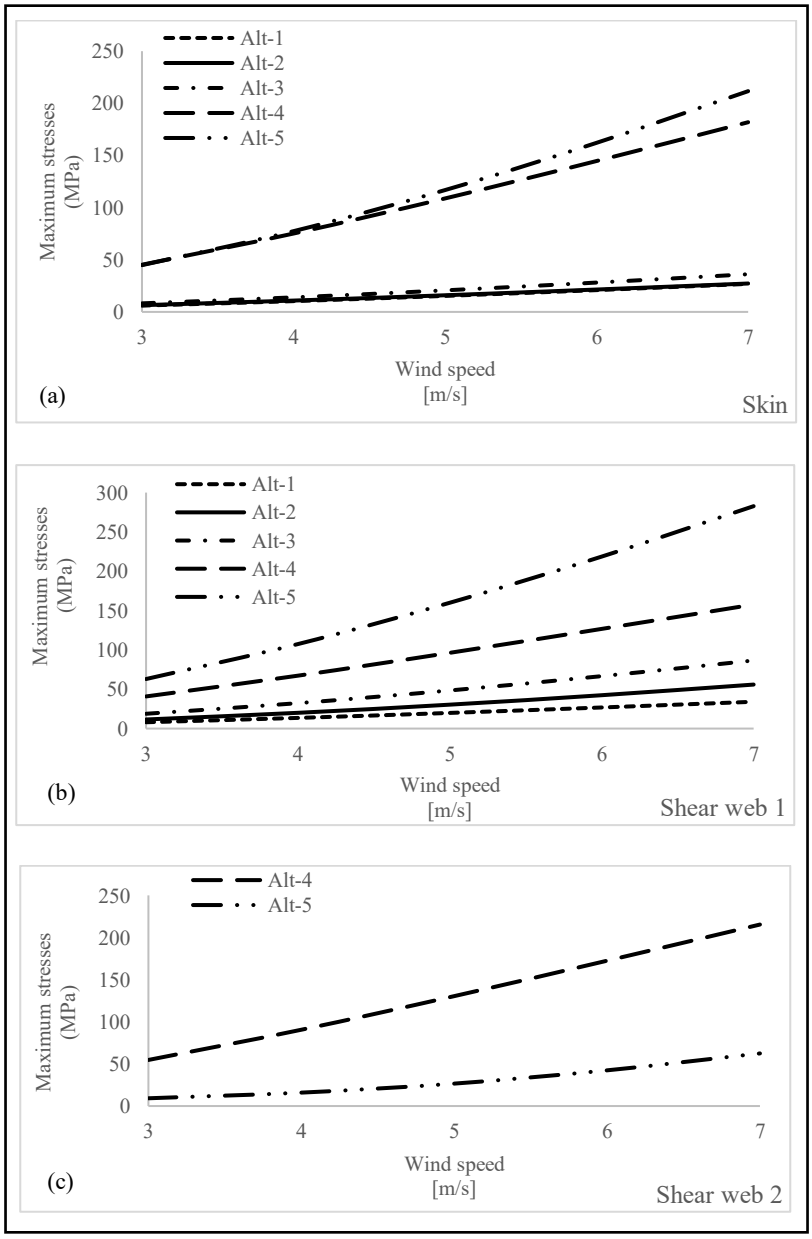


Figure 12. Maximum stress on the skin (a), shear web-1 (b), and shear web-2 (c)

### *3.2 Dynamic modal analysis*

Figure 13 illustrates the evolution of modal frequencies (modes 1 (a), mode 2 (b), mode 3 (c), and mode 4 (d) across five different shear web design alternatives (Alt-1 through Alt-5) as a function of wind speed, together with the corresponding natural frequencies of the unloaded blade. Across the evaluated designs and the whole operational wind speed range, the modal frequencies of the loaded blades consistently remain well above the likely excitation frequencies that may result from rotor rotation or aerodynamic disturbances. This pronounced separation provides a critical operational safety margin, substantially minimizing the potential for resonant amplification during regular turbine operation.

A detailed examination of the curves confirms that none of the analysed blade configurations demonstrate modal frequencies that intersect the range of operational excitation, highlighting a very low risk of resonance. Alt-2 shows the highest modal frequencies at each mode among the alternatives, suggesting a more robust and structurally rigid system. The capacity to maintain modal frequencies safely detached from primary excitation sources is fundamental for ensuring the structural integrity, mitigating fatigue, and prolonging the service life of the blade.

Further supporting this, Figure 13 presents additional results from the dynamic modal analysis. The data show that, for mode 1, Alt-5 yields the lowest frequency, while for modes 2, 3, and 4, Alt-4 yields the lowest frequency. The presence of two broadly distributed shear webs in both Alt-4 and Alt-5 appears to impart a greater resistance to dynamic excitation, as compared to designs with only a single shear web. However, the disparity in modal frequency between these two designs is minor, suggesting both are potentially viable candidates for horizontal-axis wind turbine blade applications. Notably, as also discussed by Sharma *et al*. (2021), the number of shear webs exerts relatively little influence on the modal frequencies, as evidenced by the similar frequency values observed across modes 1 to 4.

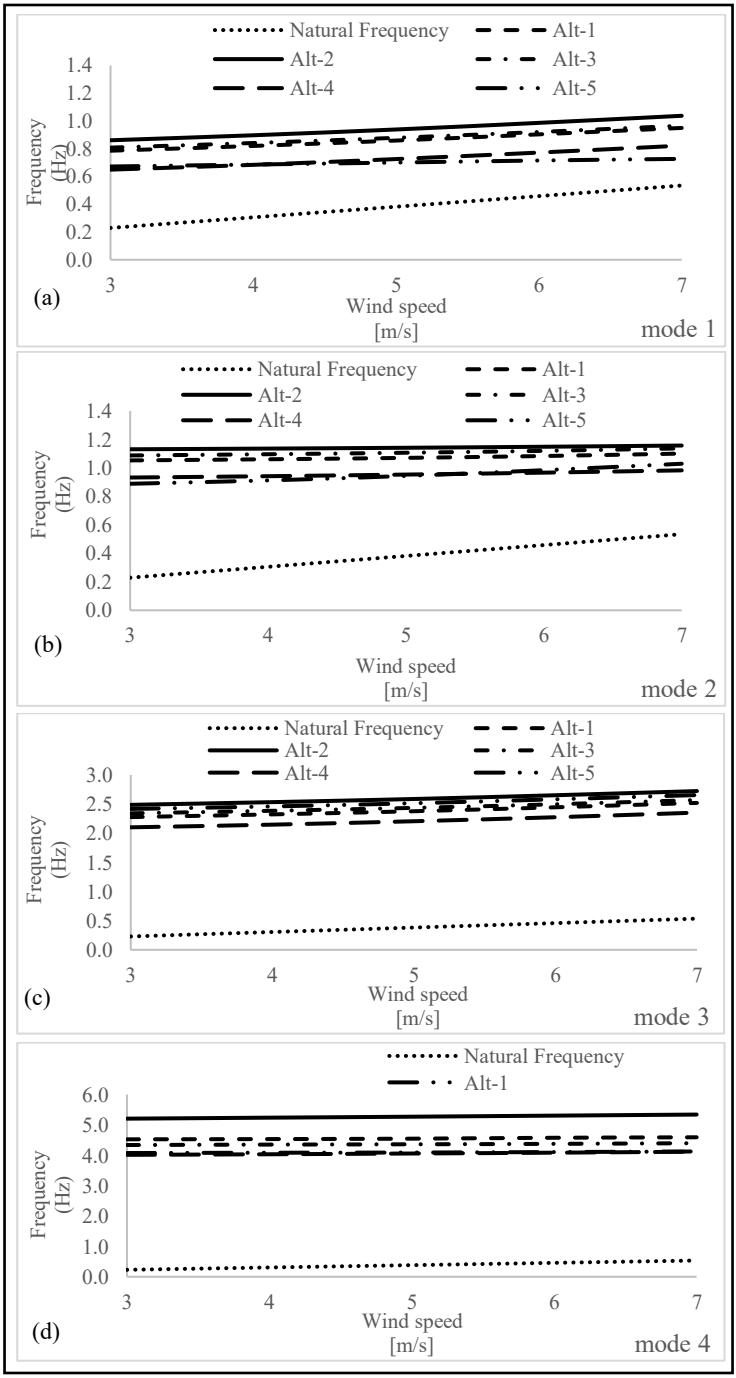


Figure 13. Frequencies: mode 1 (a); mode 2 (b); mode 3 (c); mode 4 (d)

In summary, the modal analysis underscores that these optimized shear web configurations are structurally sound and provide ample safety against resonance throughout the investigated operational envelope, thus supporting their suitability for practical wind turbine blade deployment.

### *3.3 Validation*

In engineering and simulation-based design, validation of results is essential to ensure that the chosen approach accurately represents real-world conditions. This study conducted internal validation by comparing two numerical approaches—an analytical method based on the Finite Element Method (FEM) and Computational Fluid Dynamics (CFD) simulations—for stress and structural deflection analysis of alternative blade 2 within a freestream wind speed range of 3–7 m/s.

#### 3.3.1 Surface stress analysis validation

Figure 14 presents the comparison of surface stress between the two methods. The stress values obtained from CFD were consistently higher than those from the analytical method, with the relative margin of error increasing from 14.29% at 3 m/s to 22.41% at 7 m/s. This indicates that CFD simulations can capture dynamic effects and airflow complexities more comprehensively, especially at higher wind speeds. Therefore, while the analytical (FEM) method is effective as an initial approach, CFD is recommended for analyses requiring high accuracy in stress calculations resulting from aerodynamic loads.

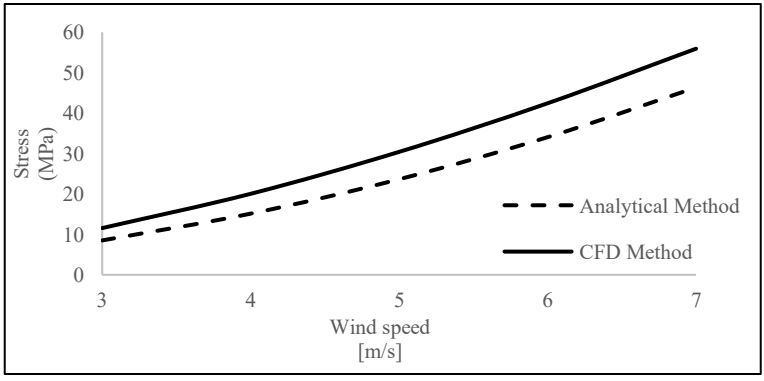


Figure 14. Validation of stress

3.3.2 Deflection analysis validation

Figure 15 illustrates the relationship between wind speed and blade structural deflection. Both methods showed similar trends, with deflection increasing as wind speed rises. However, CFD simulations consistently produced slightly higher deflection values compared to the analytical results. The relative margin of error between the methods ranged from 10.00% to 20.00%, with the highest value observed at 3 m/s and decreasing to 10% at 7 m/s. This decrease suggests that the accuracy of the analytical method approaches CFD results at higher wind speeds. This reinforces the reliability of the FEM model in predicting initial structural responses and emphasizes the importance of CFD for a more detailed analysis of deformations due to aerodynamic loads.

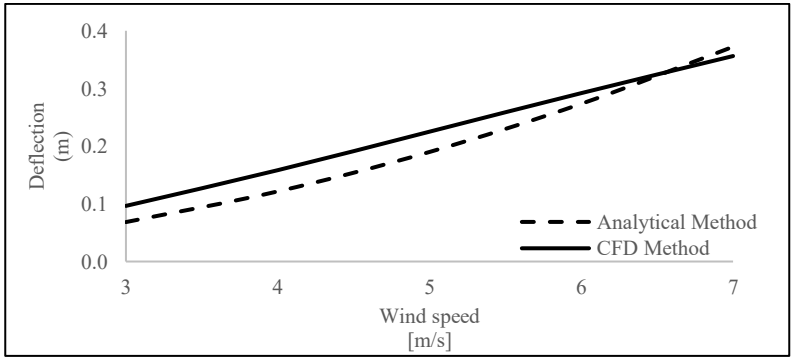


Figure 15. Validation of deflection

## 4. Conclusions and Recommendations

This study systematically analysed five alternative shear web designs for horizontal-axis wind turbine blades with a rotor diameter of 25 m, operating within a wind speed range of 3–7 m/s. The simulation results indicate that the Alt-2 configuration, featuring a short banana leaf midrib-inspired shear web, achieves the lowest deflection and stress values, as well as optimal dynamic stability. Consequently, Alt-2 is recommended as the most promising design for medium-scale wind turbines in low-wind-speed environments.

A critical evaluation of the mechanical performance revealed that biomimetic shear web configurations—particularly those inspired by both short and long

banana leaf midribs—can significantly reduce deflection and stress compared to conventional designs, while dual-web configurations further enhance dynamic stability. These findings underscore the potential of plant-inspired topologies to improve the structural efficiency and reliability of wind turbine blades under low wind speed conditions.

However, it should be noted that this study relies solely on numerical simulations (FEM and one-way FSI), and the lack of experimental verification remains a significant drawback. The accuracy of the results is nevertheless influenced by the assumptions and simplifications present in the simulation models, even though internal validation between CFD and FEM techniques supports them.

To confirm numerical predictions and evaluate the practical viability of these biomimetic designs, future research should concentrate on creating prototype blades with shear webs inspired by banana leaf midribs and performing experimental validation, such as wind tunnel or laboratory-scale testing. Further investigation into the advantages and drawbacks of plant-inspired shear web topologies in wind turbine applications will also be necessary. This includes two-way FSI analysis, fatigue life assessment, and optimization for larger-scale blades.

## 5. Acknowledgement

The authors thank Lembaga Pengelola Dana Pendidikan and the Indonesian Ministry of Finance for funding the entire doctoral education of the first author at the Bandung Institute of Technology. They also acknowledge the Bandung Institute of Technology for its assistance with the research.

## 6. References

Balokas, G., & Theotokoglou, E.E. (2018). Cross-section analysis of wind turbine blades: comparison of failure between glass and carbon fiber. *Advanced Composite Materials 27*(6), 561–574. https://doi.org/10.1080/09243046.2017.1405602

Det Norske Veritas, & Risø National Laboratory. (2002). Guidelines for design of wind turbines (2nd ed.). DNV/Risø.

Ennos, A.R., Spatz, H.C., & Speck, T. (2000). The functional morphology of the petioles of the banana, Musa textilis. *Journal of Experimental Botany 51*(353). Oxford University Press: 2085–2093. https://doi.org/10.1093/jexbot/51.353.2085.

Hayat, K., Siddique, S., Sultan, T., Ali, H.T., Aloufi, F.A., & Halawani, R.F. (2022). Effect of spar design optimization on the mass and cost of a large-scale composite wind turbine blade. *Energies, 15*(15), 5612. https://doi.org/10.3390/en15155612

Liu, J.W., Liu, P.F., Leng, J.X., & Wang, C.Z. (2022). Finite element analysis of damage mechanisms of composite wind turbine blade by considering fluid/solid interaction. Part I: Full-scale structure. *Composite Structures, 301*, 116212. https://doi.org/10.1016/j.compstruct.2022.116212

Liu, W., & Gong, J. (2011). Adaptive bend-torsional coupling wind turbine blade design imitating the topology structure of natural plant leaves. In: Al-Bahadly, I. (Eds.), *Wind Turbines* (pp. 51-86). London, United Kingdom: InTech. https://doi.org/10.5772/14804

Liu, W., Gong, J, Liu, X., & Zhang, C. (2009). A kind of innovative design methodology of wind turbine blade based on natural structure. In: IEEE, *2009 Second International Conference on Information and Computing Science*, Manchester, UK, 350–354. https://doi.org/10.1109/ICIC.2009.399

Liu, W., Ma, Y., Wang, N., Luo, Y., & Tang, A. (2022). A design of composite spar/shear web with ZPR honeycombs and graded structures for wind turbine blades. *Mechanics of Advanced Materials and Structures, 29*(25), 3633–3645. https://doi.org/10.1080/15376494.2021.1907004

Momeni, F., Sabzpoushan, S., Valizadeh, R., Morad. M.R., Liu, X., & Ni, J. (2019). Plant leaf-mimetic smart wind turbine blades by 4D printing. *Renewable Energy, 130*, 329–351. https://doi.org/10.1016/j.renene.2018.05.095

Nebiewa, A.M., Abdelsalam, A.M., Sakr, I.M., El-Askary, W.A., Abdalla, H.A., & Ibrahim, K.A. (2026). Static load and structural analysis of a small horizontal axis wind turbine blade: Experimental and theoretical studies using the fluid-structure interaction method. *Renewable Energy, 256*(Part F), 124385. https://doi.org/10.1016/j.renene.2025.124385

Omidvarnia, F., & Sarhadi, A. (2024). Nature-inspired designs in wind energy: A review. *Biomimetics, 9*(2), 90. https://doi.org/10.3390/biomimetics9020090

Rosa F., Soetikno P., Suweca I.W., & Moelyadi M.A. (2022). A new airfoil based on banana leaf midrib morphology for horizontal axis wind turbine. IOP Conference Series: *Earth and Environmental Science, 1108*(1), 012001. https://doi.org/10.1088/1755-1315/1108/1/012001

Rosa, F., Soetikno, P., Suweca, I.W., & Moelyadi, M.A. (2022). Geometric morphometric banana leaf midrib as wind turbine airfoil profile. *Jurnal Mekanova: Mekanikal, Inovasi dan Teknologi, 8*(2), 213–224. https://doi.org/10.35308/jmkn.v8i2.6095

Rosa, F., Soelaiman, D.T.A.F., Soetikno, P., Suweca, I.W., & Moelyadi, M.A. (2025). New profile based on plant to increase $Cp$ for medium horizontal axis wind turbine. *CFD Letters, 17*(9), 81–103. https://doi.org/10.37934/cfdl.17.9.81103.

Sharma, T., Choudhury, S., Murari, V., & Shukla, K.K. (2021). The effect of shear web on the dynamic response of a wind turbine blade subjected to actual dynamic load. *Journal of Materials: Design and Applications, 235*(8), 1868–1878. https://doi.org/10.1177/14644207211015264.

Wang-yu, L., & Yong, Z. (2010). Network study of plant leaf topological pattern and mechanical property and its application. *Advances in Natural Sciences, 3*(2), 82–92. http://doi.org/10.3968/j.ans.1715787020100302.009

Wolff-Vorbeck, S., Langer, M., Speck, O., Speck, T., & Dondl, P. (2019). Twist-to-bend ratio: An important selective factor for many rod-shaped biological structures. *Scientific Reports, 9*, 17182. https://doi.org/10.1038/s41598-019-52878-z

Yang, H., Chen, J., Pang, X., & Chen, G. (2019). A new aero-structural optimization method for wind turbine blades used in low wind speed areas. *Composite Structures, 207*, 446–459. https://doi.org/10.1016/j.compstruct.2018.09.050

Zhang, Z., Zhang, C., Qiao, Y., Zhou, Y., & Wang, S. (2023). Design and mass optimization of numerical models for composite wind turbine blades. *Journal of Marine Science and Engineering, 11*(1), 75. https://doi.org/10.3390/jmse11010075

Zhu, J., Cai, X., & Gu, R. (2016). Aerodynamic and structural integrated optimization design of horizontal-axis wind turbine blades. *Energies, 9*(2), 66. https://doi.org/10.3390/en9020066

Zhu, J., Zhou, Z., & Cai, X. (2020). Multi-objective aerodynamic and structural integrated optimization design of wind turbines at the system level through a coupled blade-tower model. *Renewable Energy, 150*, 523–537. https://doi.org/10.1016/j.renene.2020.01.013